

The combination of neutron spin echo and dielectric spectroscopy to examine tube dilation

Paula Malo de Molina^{1,2}, *Angel Alegría*^{1,3}, *Jürgen Allgaier*⁴, *Margarita Kruteva*⁴, *Ingo Hoffmann*⁵, *Sylvain Prévost*⁵, *Michael Monkenbusch*⁴, *Dieter Richter*⁴, *Arantxa Arbe*¹, and *Juan Colmenero*^{1,3,6*}

¹Materials Physics Center (MPC), Centro de Física de Materiales (CFM) (CSIC-UPV/EHU), Paseo Manuel de Lardizabal 5, 20018 San Sebastián, Spain

²IKERBASQUE-Basque Foundation for Science, Euskadi Plaza 5, 48009 Bilbao, Spain

³Departamento de Polímeros y Materiales Avanzados: Física, Química y Tecnología, University of the Basque Country (UPV/EHU) PO Box 1072, 20018 Donostia, Spain

⁴Jülich Centre for Neutron Science, Forschungszentrum Jülich GmbH, 52425 Jülich, Germany

⁵Institut Laue-Langevin, 71 Avenue des Martyrs, CS 20156, Cedex 9 38042 Grenoble, France

⁶Donostia International Physics Center, Paseo Manuel de Lardizabal 4, 20018 Donostia, Spain

Abstract. The polymer dynamics in blends of long and short chains spans several decades in time and the understanding of the effect of the short chains on the relaxation mechanism of the long chains due to constraint release requires the combination of microscopic and macroscopic techniques. While the long-time dynamics can be accessed by mechanical or dielectric spectroscopy (DS), its relation to the microstructural details requires the application of theoretical models. In contrast, neutron spin echo (NSE) measures directly the dynamic structure factor reflecting the process of constraint removal at the molecular scale. Here the comparison of NSE and DS results in a model blend of short and long polyisoprene enables the exploration of the entire time regime showing that constraint release leads to a dilation of the confining tube. We show the description of the dynamic tube dilation using a simple model in which the time controlling the tube dilation for the long chain is the terminal time of the short chain.

1 Introduction

In polymer materials, additives are typically used to modify their mechanical properties or improve processability. In particular, the addition of small molecules to high molecular weight entangled polymers leads to lower viscoelasticity, which is very relevant in blends and polydisperse polymers. In general, the long-time dynamics of well-entangled linear monodisperse chains in the melt is well understood in terms of the tube model proposed by Edwards and De Gennes [1,2]. In this ideal tube model the surrounding chains act as topological constraints and confine the probe chain into a tube region, which restricts the lateral motion of the chain within its diameter, d . Then, the probe chain relaxes by reptation. However, in real systems other mechanisms compete with reptation, mainly contour length fluctuations (CLF), i.e., fluctuations of the length of the tube, and constraint release (CR), which refers to the probe chain motions induced by the motions of the surrounding chains [3,4].

Binary polymer blends composed of two monodisperse components with the same chemistry (isofrictional blends) and architecture, are simplified model systems to investigate the effect of polydispersity [5–13]. CR effects are more important in binary blends

of short and long chains, where the rapid motions of the short chains release the constraints on the long chain, allowing the latter to relax faster than it would by its own reptation mechanism. Thus, the tube that confines the long chain reorganizes as a consequence of the release of constraints. This process can be, in principle, modelled by assuming Rouse-like motion of the tube, where the segmental motion is replaced by individual CR-events [14]. On the other hand, a simplified representation of the many-chain CR effects is the so-called dynamic tube dilation (DTD), where the diameter of the tube confining the long chain increases with time due to CR. The concept of the DTD was first proposed by Marrucci [15] for homopolymer monodisperse melts where the portion of the chain that has escaped from its original tube can act as a solvent for the remaining tube sections.

Most of the experimental studies of CR effects in polymer blends are carried out with macroscopic rheological or dielectric techniques, focusing on the terminal regime of the viscoelastic behavior. Yet, within a DTD mechanism, the tube should already have reached its final dilated value at that time-regime. Therefore, the time dependence of the CR or DTD mechanism at molecular level is little known. Some molecular dynamics (MD)-simulations studies have attempted to address this problem from a molecular

* Corresponding author: juan.colmenero@ehu.eus

point of view [16,17]. In a recent study [18] we have shown that the time-dependent tube dilation in isofrictional polymer blends can be directly observed by neutron spin echo (NSE) as an additional time dependence of the dynamic structure factor in the local reptation regime. By combining NSE with DS, we could identify the characteristic time driving tube dilation as the terminal time of the short component of the blend.

In general, the dynamic process of tube reptation occurs over a very wide range of time scales, which requires not only the time and length scale resolution provided by neutron spectroscopy but also the combination with other macroscopic techniques. In particular, dielectric spectroscopy in combination with neutron spectroscopy has been very helpful to shed light on the dynamic mechanisms of many systems such as water [19]. In this article, we show the dynamics of entangled chains blended with shorter chains along the entire time regime by combining NSE and DS.

2 Experimental

The single-chain dynamics of a polymer chain can be measured with neutron spin echo by selectively H-labelling a small part of the long chains immerse in a matrix of deuterated polymers. Nearly monodisperse long and short linear polyisoprene were synthesized by anionic polymerization. The molecular weight of the polymers were : $M_w = 83.5$ kDa and PDI=1.01 (long hPI); $M_w = 90.2$ kDa and PDI=1.03 (long dPI); $M_w = 12.4$ kDa and PDI=1.04 (short dPI). The entanglement mass of PI is $M_e \approx 5$ kg/mol. Long-linear PI had $Z = M/M_e \approx 16$ entanglements per chain while the short-linear PI had $Z = 2.4$. The samples for neutron scattering experiments contained 10% of long protonated PI chains in the otherwise deuterated material. The NSE data were obtained in IN15 (ILL, Grenoble, France) [20]. A broadband dielectric spectrometer, Novocontrol Alpha analyzer, was used to measure the complex dielectric permittivity.

3 Results

Figure 1 shows the normalized chain dynamic structure factor $S(Q,t)/S(Q,0)$ corresponding to long chains in the melt and in the blend with the small linear additive (with a total long chain volume fraction $\phi_L = 0.5$) that were previously reported [18]. In both cases, the curves are characterized by a first decay at short times, related to motions of the chain within the tube, followed by a plateau characteristic of confinement. The Q -dependence of this plateau is related to the confining geometry, in this case the tube.

The dynamic structure factor of entangled polymers can be described in terms of the De Gennes model [21]:

$$\frac{S(Q,t)}{S(Q,0)} = \left[1 - \exp\left(-\frac{Q^2 d^2}{36}\right) \right] S^{loc}(Q,t) + \exp\left(-\frac{Q^2 d^2}{36}\right) S^{esc}(Q,t) \quad (1)$$

where $S^{loc}(Q,t)$ and $S^{esc}(Q,t)$ are related to the local reptation and escape process from the tube (creep motion), respectively. Generally, in the time window covered by NSE it can be assumed that $S^{esc}(Q,t) \approx 1$. We will show later that this is a good approach also in our case. On the other hand, $S^{loc}(Q,t)$ might be approximated by a phenomenological stretched exponential function. Then, the expression for the dynamic structure factor is reduced to:

$$\frac{S(Q,t)}{S(Q,0)} = \left[1 - \exp\left(-\frac{Q^2 d^2}{36}\right) \right] \exp\left[-\left(\frac{t}{\tau}\right)^\beta\right] + \exp\left(-\frac{Q^2 d^2}{36}\right) \quad (2)$$

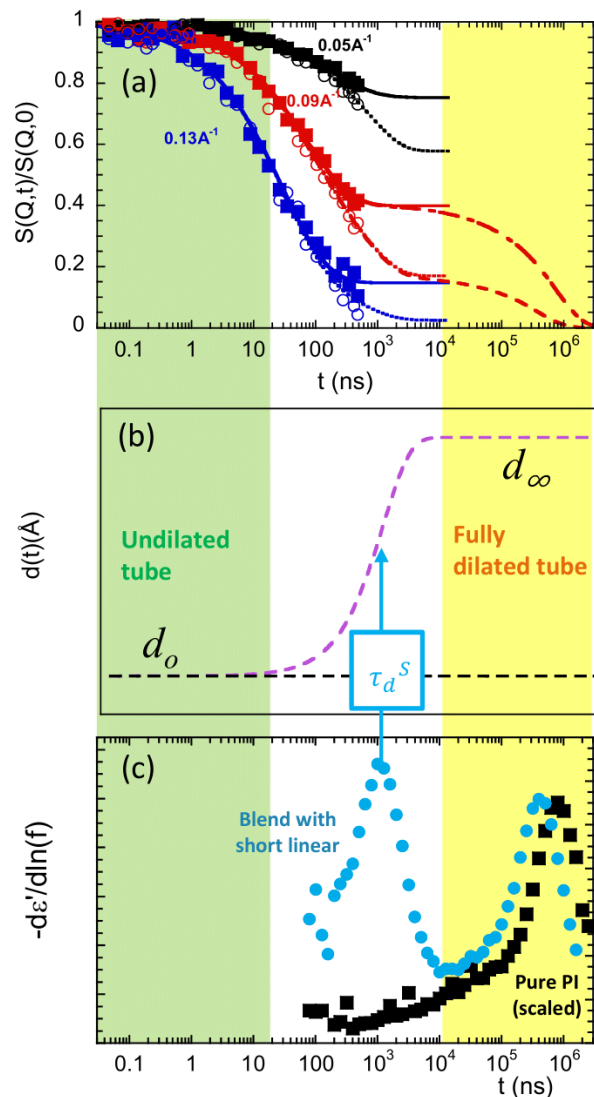


Fig. 1. **a)** Single-chain dynamic structure factor measured by NSE of long-PI chains in bulk (filled symbols) and in blends with short linear (empty symbols) at $\phi_L = 0.5$ and the three values of the scattering vector indicated. Lines are fits as explained in the text. **b)** Time dependence of the tube diameter. **c)** Normalized natural-log frequency (f) derivative of the real part of the dielectric permittivity as a function of the time variable $t = 1/(2\pi f)$. All results correspond to 423 K.

Using eq. 2 to model the $S(Q,t)/S(Q,0)$ of the pure long chains (solid lines in Figure 1a), we obtain a value

of the effective tube of $d_0 = 64 \text{ \AA}$ — in good agreement with the values reported for polyisoprene [22]. We explicitly refer to this tube diameter as effective since it includes all effects of CR, CLF, etc. taking place in the homopolymer. This is our reference value.

The comparison between the data of the long/short blend and pure long melt reveals that the dynamic structure factor of the long chain is unaffected by the presence of the additives at times shorter than ~ 100 ns. At about 100 ns, a progressively more pronounced decay of $S(Q, t)/S(Q, 0)$ is observed for long chains in the blends with respect to the pure long chains. Yet, the decay does not reveal a significant tube dilation. This suggests that up to 100 ns the confinement is the same in both systems and the tube starts to dilate at around 100 ns. Incidentally, this time is close to the entanglement time of polyisoprene, $\tau_e = 90$ ns at 423K.

If the additives were small (or fast) enough, the tube would be expected to be fully dilated in the NSE time window and the tube diameter obtained from eq. 2 and from macroscopic spectroscopy techniques should agree [23]. Here, the short chains are twice the entanglement molar mass, and NSE shows that the tube barely starts dilating within the accessible time window. Thus, to probe the tube dilation it is necessary to measure the long-time behavior with macroscopic relaxation techniques. In the case of polyisoprene that has both local dipole moments parallel and perpendicular to the chain backbone, the terminal relaxation range can be nicely assessed by dielectric spectroscopy (DS) through the so-called “normal mode” [24]. This relaxation reflects the fluctuations of the end-to-end vector of the chains and therefore it directly reveals the disentanglement time, which is related to the tube diameter with the tube theory.

Generally, DS results are measured as a function of frequency but, to compare with NSE, here it is more convenient to represent the data in terms of the time ($t = 1/(2\pi f)$). Figure 1c shows the time-dependence of the derivative of the real part of the complex dielectric permittivity, $d\epsilon'(f)/d\ln(f)$, with $\ln f$ being the natural logarithm of the frequency f . The peaks observed in the experimental dynamic window at the high temperature explored correspond to the above introduced “normal mode”. In the case of entangled polymer melts, the maximum of this peak corresponds to the disentanglement time, τ_d . In the pure melt, only one peak is observed. By contrast, the results corresponding to the blend show two peaks: one centered at shorter time associated with the terminal time of the short polymer ($\tau_d^s = 1086$ ns) and the long-time peak related to the normal mode of the long polymer in the blend, $\tau_d(\phi_L)$. The latter is shifted to faster times compared to the long chain in its pure matrix, owing to the acceleration of τ_d in the presence of the short-chain additives.

In the tube model, the tube diameter d is related to the reptation time as $d = [3R_E^6/(\pi^2 W \ell^4 \tau_d)]^{1/2}$, where R_E is the chain end-to-end distance and $W \ell^4$ the Rouse rate. Taking into account that the blend is isofrictional (with the same $W \ell^4$) and that the conformation of the long linear chains doesn't change upon blending

(Gaussian, with $R_E = 24$ nm) [18,25], the dilated tube diameter for the long PI component in the blend relative to the diameter of the pure long PI is given by $d_\infty/d_0 = [\tau_d/\tau_d(\phi_L)]^{1/2}$. Considering the value of the undiluted tube as $d_0 = 64 \text{ \AA}$, then the fully dilated tube diameter in the blend is $d_\infty = 89 \text{ \AA}$.

Note that the dynamic structure factor of the chain in the blend cannot be described using eq. 2 with the dilated tube diameter obtained from DS. Thus, the dilation from d_0 to d_∞ happens at times between τ_e and τ_d . In dielectric spectroscopy, the effective dilation process is inaccessible because it is hidden by the normal mode relaxation of the short component. Therefore, it can only be accessed by NSE that probes the long single chain dynamic structure factor selectively. Then, in the spirit of the DTD, instead of a static tube, we use a time-dependent tube for the long PI chains in the blends growing from d_0 to d_∞ in the time range of the relaxation of the fast component of the blend. Accordingly, eq. 2 becomes:

$$\frac{S(Q, t)}{S(Q, 0)} = \left[1 - \exp\left(-\frac{Q^2 d(t)^2}{36}\right) \right] \exp\left[-\left(\frac{t}{\tau}\right)^\beta\right] + \exp\left(-\frac{Q^2 d(t)^2}{36}\right) \quad (3)$$

As a first approximation, the time dependence of the tube diameter can be considered as an exponential function $d(t) = d_\infty + (d_0 - d_\infty) \exp[-t/\tau_d^s]$ with the time constant corresponding to the terminal time of the short additive in the blend, τ_d^s , obtained from DS (see Figure 1b).

Moreover, considering that the blend is isofrictional and the short-time behavior of the NSE results is insensitive to the presence of additives, the β and τ parameters of the first term in eq. 3 were fixed to the values obtained for pure long-linear PI. The fits using eq. 3 for the blend represented by dotted lines in Figure 1a show excellent agreement with the experimental data, in particular considering that there are no fitting parameters.

We note that a similar result was also found for star additives with 8 and 18 arms, where there the time governing the tube dilution was closer to the terminal time of the additive obtained from rheological measurements [25].

Finally, we can verify the validity of neglecting the escape dynamics using eqs. 2 and 3 to describe the NSE data since we know from DS the reptation time controlling the escape process from the tube $S^{esc}(Q, t)$. For that, in Figure 1a we calculated the full curves in a representative Q -value ($Q = 0.09 \text{ \AA}^{-1}$) in an extended time window considering for the escape term the expression $S^{esc}(Q, t) = \frac{8}{\pi^2} \sum_{n-\text{odd}} \frac{1}{n^2} \exp(-n^2 t/\tau_d)$ [26]. This is obtained from the full general one given by Doi and Edwards [27] under the assumption $QR_E \gg 1$. The full model is represented by the dashed lines in Figure 1a showing that they overlap with eqs. 2 and 3 up to $\sim 3 \cdot 10^5$ ns both in the case of the pure long polymer and the blend. In this way, we demonstrate that within the NSE time window ($t < 480$ ns), the expression $S^{esc}(Q, t) \equiv 1$ is valid.

4 Conclusions

The combination of neutron spin echo with dielectric spectroscopy in isofrictional polymer blends of short and long polyisoprene chains shows that at short times the tube is unaltered and at long times it is dilated. NSE can directly probe the process of time-dependent constraints removal at molecular scale. A model of dynamic tube dilation describes the NSE experimental data using the parameters obtained from dielectric spectroscopy showing that the time at which the tube dilates is the terminal time of the additive.

The authors acknowledge the financial support received from the IKUR Strategy under the collaboration agreement between Ikerbasque Foundation and Materials Physics Center on behalf of the Department of Education of the Basque Government. Financial support by MCIN/AEI/10.13039/501100011033 and “ERDF – A way of making Europe” (PID2021-123438NB-I00) and Eusko Jaurlaritz – Basque Government (IT1566-22).

References

1. S. F. Edwards, Proc. Phys. Soc. **91**, 513 (1967)
2. P. G. de Gennes, J. Chem. Phys. **55**, 572 (1971)
3. J. Klein, Macromolecules **11**, 852 (1978)
4. M. Daoud, P. G. De Gennes, J. Polym. Sci. Polym. Phys. Ed. **17**, 1971 (1979)
5. S. Wang, S.-Q. Wang, A. Halasa, W.-L. Hsu, Macromolecules **36**, 5355 (2003)
6. H. Watanabe, S. Ishida, Y. Matsumiya, T. Inoue, Macromolecules **37**, 6619 (2004)
7. H. Watanabe, Y. Matsumiya, E. van Ruymbeke, Macromolecules **46**, 9296 (2013)
8. M. E. Shivokhin, E. van Ruymbeke, C. Bailly, D. Kouloumasis, N. Hadjichristidis, A. E. Likhtman, Macromolecules **47**, 2451 (2014)
9. P. S. Desai, B.-G. Kang, M. Katarova, R. Hall, Q. Huang, S. Lee, M. Shivokhin, T. Chang, D. C. Venerus, J. Mays, J. D. Schieber, R. G. Larson, Macromolecules **49**, 4964 (2016)
10. T. Ebrahimi, H. Taghipour, D. Griebel, P. Mehrkhodavandi, S. G. Hatzikiriakos, E. van Ruymbeke, Macromolecules **50**, 2535 (2017)
11. T. Shahid, Q. Huang, F. Oosterlinck, C. Clasen, E. van Ruymbeke, Soft Matter **13**, 269 (2017)
12. H. Lentzakis, S. Costanzo, D. Vlassopoulos, R. H. Colby, D. J. Read, H. Lee, T. Chang, E. van Ruymbeke, Macromolecules **52**, 3010 (2019)
13. R. Hall, B.-G. Kang, S. Lee, T. Chang, D. C. Venerus, N. Hadjichristidis, J. Mays, R. G. Larson, Macromolecules **52**, 1757 (2019)
14. D. J. Read, M. E. Shivokhin, A. E. Likhtman, J. Rheol. (N. Y. N. Y.) **62**, 1017 (2018)
15. G. Marrucci, J. Polym. Sci. Polym. Phys. Ed. **23**, 159 (1985)
16. Z. Wang, R. G. Larson, Macromolecules **41**, 4945 (2008)
17. M. Langeloth, Y. Masubuchi, M. C. Böhm, F. Müller-Plathe, J. Chem. Phys. **141**, 194904 (2014)
18. P. Malo de Molina, A. Alegría, J. Allgaier, M. Kruteva, I. Hoffmann, S. Prévost, M. Monkenbusch, D. Richter, A. Arbe, J. Colmenero, Phys. Rev. Lett. **123**, 187802 (2019)
19. A. Arbe, P. Malo de Molina, F. Alvarez, B. Frick, J. Colmenero, Phys. Rev. Lett. **117**, 185501 (2016)
20. M. Kruteva, B. Farago, I. Hoffmann, P. Malo de Molina, *Data for “Influence of the Topology on the Polymer Dynamics: Blends of Long Linear Polymer Chains with Shortlinear and Star-like Polymers”* <https://doi.org/10.5291/ILL-DATA.CRG-2462> (Institut Laue-Langevin, Grenoble, 2018)
21. P. G. De Gennes, J. Phys. **42**, 735 (1981)
22. L. J. Fetters, D. J. Lohse, D. Richter, T. A. Witten, A. Zirkel, Macromolecules **27**, 4639 (1994)
23. B. J. Gold, W. Pyckhout-Hintzen, A. Wischnewski, A. Radulescu, M. Monkenbusch, J. Allgaier, I. Hoffmann, D. Parisi, D. Vlassopoulos, D. Richter, Phys. Rev. Lett. **122**, 088001 (2019)
24. C. Riedel, A. Alegría, P. Tordjeman, J. Colmenero, Rheol. Acta **49**, 507 (2010)
25. P. Malo de Molina, A. Alegría, J. Allgaier, M. Kruteva, I. Hoffmann, S. Prévost, M. Monkenbusch, D. Richter, A. Arbe, J. Colmenero, Macromolecules **53**, 5919 (2020)
26. D. Richter, M. Monkenbusch, A. Arbe, J. Colmenero, Neutron Spin Echo in Polymers Systems, Advances in Polymer Science **174** (Springer, Berlin, Heidelberg, New York, 2005)
27. M. Doi, S. F. Edwards, The Theory of Polymer Dynamics (Clarendon, Oxford, 1986)